Pergamon

Continental Shelf Research, Vol. 16, No. 3, pp. 335–351, 1996

0278–4343/96 $9.50 + 0.00

0278–4343(95)00014–3

The Patos Lagoon summertime circulation and dynamics

OSMAR O. MOLLER JR,* JOÃO A. LORENZZENTTI,†
JOSÉ L. STECH† and MAURICIO M. MATA*

(*Received* 10 *May* 1993; *in revised form* 15 *December* 1993; *accepted* 29 *December* 1994)

Abstract—The main aspects of the summertime circulation and dynamics of the Patos Lagoon, a system located in southern Brazil and considered as one of the world's largest choked coastal lagoons, are studied through the analysis of time series of wind stress, water level and freshwater discharge, combined with the results of a barotropic circulation model. The longitudinal wind component has been verified as the main driving force, generating a set-up/set-down mechanism of oscillation with the nodal line in the midlagoon area. The period of this oscillation coincides with the passages of frontal systems for this region. The sea breeze acts as a secondary effect, being clearly observed in the northern part of the lagoon. Freshwater discharge is expected to cause variations in water level on the seasonal band and to a lesser degree in the 8–15 day time-scale. The tidal signal is of importance only near the exit to the ocean, being strongly reduced in the interior of the lagoon. Model results suggest a wind set-up momentum balance in the longitudinal direction in the deeper parts of the lagoon; near the margins, the longitudinal momentum balance is mostly of frictional form, with the wind stress being balanced by the bottom friction. In the lateral direction, a geostrophic balance is verified in both regions. The wind forced circulation is characterized by the presence of several cells with downwind velocity near the margins and upwind return flow occurring in the central areas.

1. INTRODUCTION

The Patos Lagoon, one of the largest coastal lagoons in the world, is located in the southern Brazilian coastline, between 30° S and 32° S latitude (Fig. 1). With a length of 250 km and an average width of 40 km, the lagoon has an area of 10,360 km^2. Due to an average depth of 5 m, it can be classified as a shallow lagoon. The morphology of this water body, which has a NE–SW orientation, is marked by many "cells" or "pools" limited by shallow sand spits, and as with many other coastal lagoons, it is connected to the ocean through a narrow channel of 1–2 km width and 20 km of length. Kjerfve (1986) has classified Patos Lagoon as a choked coastal lagoon, where the astronomical tides are of reduced importance and the circulation is driven by the wind and freshwater discharge. According to Herz (1977) the astronomical tide at Rio Grande is one of the mixed type with a diurnal dominance. The mean and maximum amplitude values are 0.5 and 1.2 m, respectively.

*Fundação Universidade do Rio Grande–FURG, Laboratorio de Oceanografia Física, Depto. de Física, Brazil.

†Instituto Nacional de Pesquisas Espacais–INPE, Divisão de Sensoriamento Remoto, Brazil.

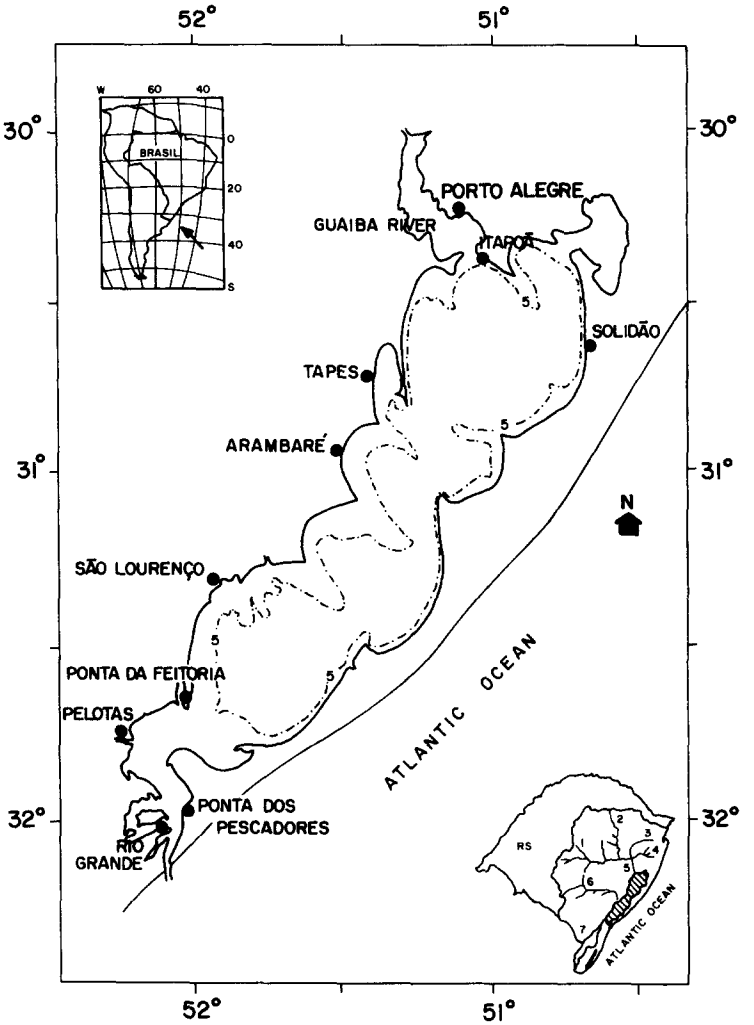

Fig. 1. The Patos Lagoon, showing the main locations referred in the text. The bottom right picture shows the lagoon hydrographical basin formed by the following tributaries: Jacuí (1), Taquarí (2), Sinos (3), Caí (4), Guaíba (5) and Camaquã (6) rivers; the Mirim lake (7). The dashed line represents the 5 m isobath.

Patos Lagoon drains a 140,000 km^2 hydrological basin (Fig. 1) which receives a seasonal rainfall and exhibits an associated freshwater discharge peak in the winter (June–August) or spring (September–November). Monthly means based on 14 years of data, for the Jacui–Taquari and Camaquã rivers, varied from 500 m^3 s^{-1} in March up to 3000 m^3 s^{-1} between August and October (Bordas *et al.*, 1984). Values ranging from 500 m^3 s^{-1} up to 12,000 m^3 s^{-1}, this one related with 1982–1983 "El Nino" phenomenon, were observed by Moller *et al.* (1991).

Malaval (1922) and Motta (1969) presented some analyses of the lagoon's response to wind forcing. Their results showed that NE winds can contribute to seaward flow, while southerly winds, mainly those from SW, can produce the opposite effect. The NE winds

are dominant throughout the year, but southerly winds become more important in autumn and winter, when the frontal systems penetrate the region more frequently.

Closs (1962) has suggested that the estuarine zone limit is located around the Ponta da Feitoria region (Fig. 1), 70 km distant from the entrance. For very dry seasons and southerly winds, this limit can be displaced northward, but during flood periods it is restricted to the entrance. Moller *et al.* (1991) have observed that riverine freshwater discharge into the lagoon in excess of 3000 $m^3 s^{-1}$ can displace the mixture zone to the adjacent inner shelf. Calliari (1980) observed that the three types of estuarine circulation proposed by Cameron and Pritchard (1963) can occur in this lagoon. The well-mixed type is predominantly found during weak river flows or during strong southerly wind stress events.

The purpose of this paper is to contribute to a better understanding of the summertime response of the Patos Lagoon to wind, freshwater discharge and astronomical tidal forcing. This study was made through the analysis of some time series of field data and from the results of a barotropic numerical circulation model implemented for the region. The specific case of the three-dimensional estuarine circulation is beyond the scope of this paper, since the focus here is on the overall characteristics of the entire lagoon.

2. DATA PROCESSING AND ANALYSIS

2.1. *The observations*

Time series of water level and wind vector data were recorded at hourly intervals at the stations presented in Fig. 1. For summertime conditions, two data sets of simultaneous observations were available. The first set consisted of water level records obtained from 15 December 1987 to 27 January 1988 in Rio Grande, Arambaré and Itapoã. Wind speed and direction at Solidão and water level at Rio Grande and Itapoã, from 12 February to 28 March 1988, formed the second data set. Freshwater discharge for the Guaiba river was obtained by summing the contribution from each one of its tributaries. The rating curve method of Jacob and Kazimier (1989) has been used to convert water levels into discharge rates.

2.2. *Data processing*

Wind vector time series were decomposed into longitudinal (y) and transverse (x) components, through a 37° clockwise axis rotation from true north, making the y-component parallel to the main axis of the lagoon.

Visual analysis of the time series was used to detect bad data. Only those cases well above background noise were eliminated. A linear interpolation scheme was used to fill the voids. For those situations in which only the low frequency variations were of interest, a Lanczos-squared low pass filter was used to remove periods shorter than 40 h.

3. THE NUMERICAL MODEL

The model used in this investigation was formulated by Wang and Connor (1975) and is a one-layer barotropic, two-dimensional f-plane model, which uses the finite element technique to solve the dynamical equations of motion. The formulation is based on the

Navier–Stokes equations for the conservation of momentum and continuity equation for the conservation of mass of a fluid in rotation. The coordinate system is Cartesian, has its origin at the ocean surface with the positive x, y and z axes pointing to east, north and vertically upward, respectively. The bottom topography is a function of the x and y coordinates. The fluid system consists of one layer of constant density.

The following system of equations is obtained by vertical integration from the bottom to the free surface of the equations of momentum and continuity:

$$\frac{\partial Q_x}{\partial t} + \frac{\partial uQ_x}{\partial x} + \frac{\partial vQ_x}{\partial y} = -gH\frac{\partial \eta}{\partial x} + \frac{1}{\rho}(\tau_{wx} - \tau_{bx}) + fQ_y + F_x$$

$$\frac{\partial Q_y}{\partial t} + \frac{\partial uQ_y}{\partial x} + \frac{\partial vQ_y}{\partial y} = -gH\frac{\partial \eta}{\partial y} + \frac{1}{\rho}(\tau_{wy} - \tau_{by}) - fQ_x + F_y$$

$$\frac{\partial \eta}{\partial t} + \frac{\partial Q_x}{\partial x} + \frac{\partial Q_y}{\partial y} = 0$$

where Q_x and Q_y represent the integrated transport per unit of width for the x and y directions; u and v are the mean water column velocity components, η is the free surface elevation anomaly, ρ is the water density, τ_w is the wind stress, τ_b is the bottom stress and F represents the integrated internal stresses. The wind and bottom stresses are both parameterized using quadratic formulations of the following forms:

$$\tau_w = \rho_{\text{air}}\, C_w |U_{10}| U_{10}$$

where $C_W = (1.1 + 0.0536\, U_{10}) \times 10^{-3}$ (Wang and Connor, 1975) and U_{10} (m s^{-1}) is the wind speed 10 m above the surface;

$$\tau_b = \rho C_b |V| V$$

where $V = (u,v)$ and $C_b = 2.3 \times 10^{-3}$ (Hickey and Hamilton, 1980).

The following boundary conditions are used:

(i) a radiation condition (Orlanski, 1976) at the north and south water boundaries representing, respectively, the Guaiba river water, section (AB) and the lagoon's exit to the ocean (CD), Fig. 8;

(ii) normal flow equal to zero at the solid boundary.

4. RESULTS

4.1. *Data analysis results*

The energy spectrum of individual time series was determined through maximum entropy analysis (MEA) (Ulrich and Bishop, 1975); for Cross-Spectrum Analysis, use was made of a FFT technique (Lorenzzetti, 1976). The MEA energy spectra of unfiltered water level oscillations are shown in Fig. 2 for Rio Grande in the extreme south of the domain, Arambaré in the mid part of the lagoon and Itapoã, located in the extreme north (See Fig. 1 for locations).

One of the main characteristics shown in Fig. 2 is the high energy content of tidal components present in Rio Grande, as compared to the other places. Diurnal (D, $T = 25.6$

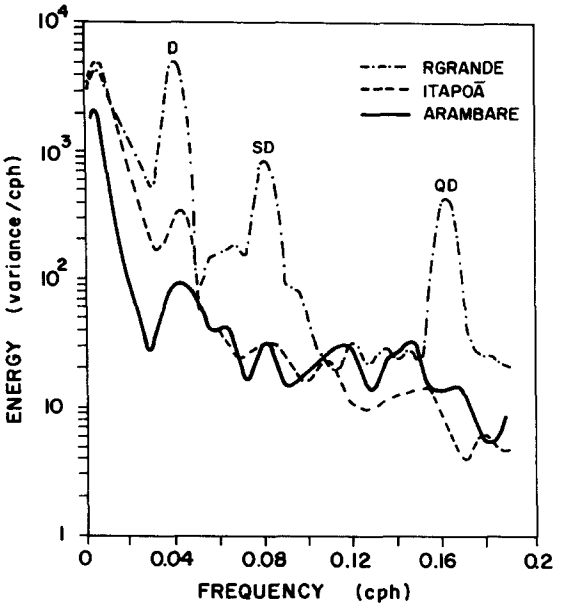

Fig. 2. Energy spectra of the water level time series recorded at Rio Grande, Arambaré and Itapoã, from 15 December 1987 to 27 January 1988.

h), semi-diurnal (SD, $T = 12.5$ h) and quarter-diurnal (QD, $T = 6.2$ h) peaks dominate the tidal frequency band for this site. It is interesting to note that the diurnal component has the same energy level as the subtidal peak and is approximately one order of magnitude stronger than the diurnal peaks observed at Itapoã and Arambaré. This strong reduction of tidal amplitude in the interior of the lagoon is a common feature observed in choked coastal systems, where the narrow channel that connects them to the ocean acts as a low-pass filter mechanism decreasing tidal amplitude (Kjerfve and Magill, 1989).

The two diurnal peaks present at Itapoã and Arambaré ($T = 24$ h) are shifted towards higher frequencies compared with that observed at Rio Grande. As indicated above, at a choked coastal lagoon like this one, the mechanism responsible for these peaks should not be of tidal origin at such distances from the entrance channel. Seiches related to the natural period of oscillation of the system could be thought of as a possible factor generating these oscillations.

In order to test this hypothesis, Defant's (1961) method was applied by dividing the lagoon into 52 cross-sections, following its longitudinal axis. The system was considered as a closed one, due to its narrow mouth. This method not only permits the determination of the natural periods of oscillation but also provides the position of the nodal line corresponding to a certain harmonic. A period of 19.3 h was obtained for the first harmonic and the nodal line was placed in the middle part of the lagoon, in the vicinity of Arambaré. The natural period hypothesis, therefore, can be disregarded and another physical mechanism must be responsible for these 24 h oscillations.

The nature of the 0.0417 cph ($T = 24$ h) peaks can be elucidated by the analysis of the spectra of the Solidão x-wind component and water level oscillations shown in Fig. 3. A sea breeze peak is noticeable at the x-wind component having the same frequency as that

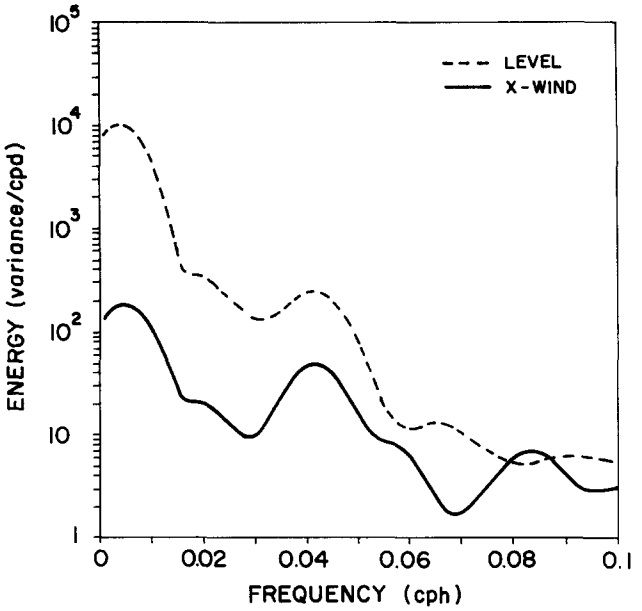

Fig. 3. Energy spectra of the *x*-wind component and water level time series for Solidão recorded from 12 February to 28 March 1988.

observed for the water level, suggesting that such oscillations are generated by the transversal wind component. A cross-spectrum analysis of both signals reveals a squared coherence of 0.59, significant at 95% level, and confirming this relationship (See Fig. 4).

For the low frequency end of the spectrum, both Rio Grande and Itapoã have almost the same energy level at the 0.0039 cph (256 h, 11 days) peak (Fig. 2). The low frequency peak for Arambaré has weaker energy levels than these other two sites (a factor of about 2.5). Figure 5 shows that the 11 day period is an evident feature, both in the filtered *y*-wind component for Solidão and in the spectra of the water level at Rio Grande and Itapoã. The cross-spectra between Itapoã water level and Solidão *y*-wind component (Fig. 6) presents a squared coherence of 0.70 for the 11 day range. Analysis of wind time series carried out by Stech and Lorenzzetti (1992) for the southern Brazilian coastline also shows the 11 day period as a dominant feature. These oscillations in the wind field are associated with the passage of the frontal systems over the area, when the prevailing northeast winds rotate to southern quadrant.

These results indicate that the longitudinal component of the wind is the main mechanism responsible for the water level oscillations along the lagoon in this frequency band. The response of the lagoon to this longitudinal wind forcing must be of the set-up/set-down type, where the piling up of water is associated with the downstream side of the wind.

To analyze the effect of the freshwater discharge of the Guaiba River system in the lagoon, spectral analysis was carried out on a data set containing four years of daily Guaiba river flow. The result of this analysis presented in Fig. 7, shows that the most significant peak is in the seasonal band (*S*). Secondary peaks with one order of magnitude less energy are present with periods ranging from 8 to 15 days. Due to the short extent of our water

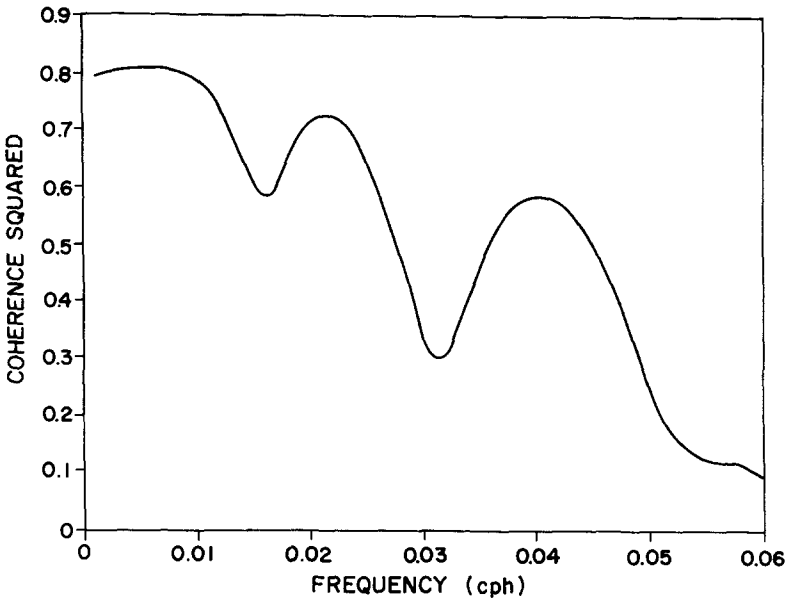

Fig. 4. Coherence squared estimates between x-wind component and water level time series recorded at Solidão.

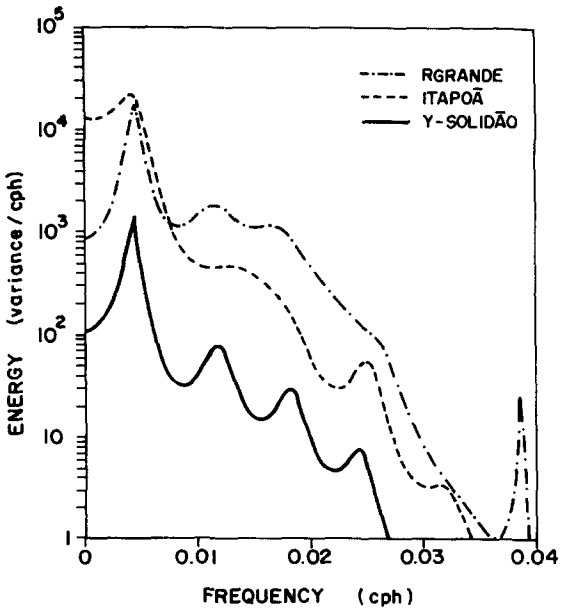

Fig. 5. Energy spectra of the Solidão y-wind component and water level time series recorded at Rio Grande and Itapoã, from 12 February to 28 March 1988.

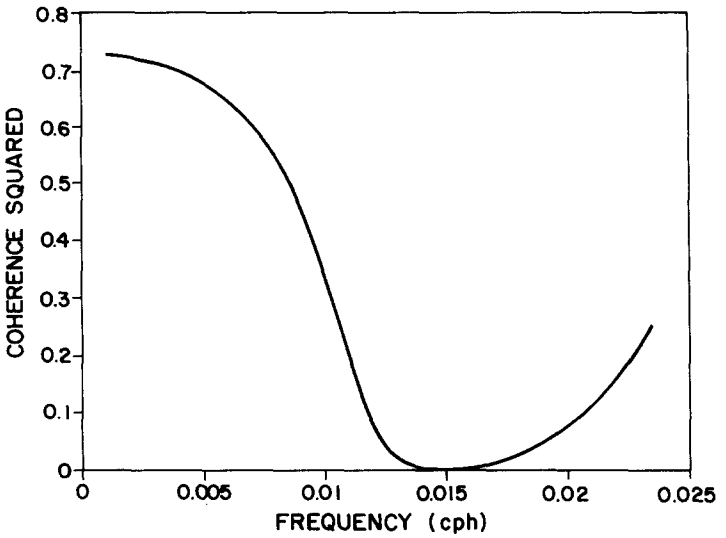

Fig. 6. Coherence estimates between Solidão *y*-wind component and Itapoã water level.

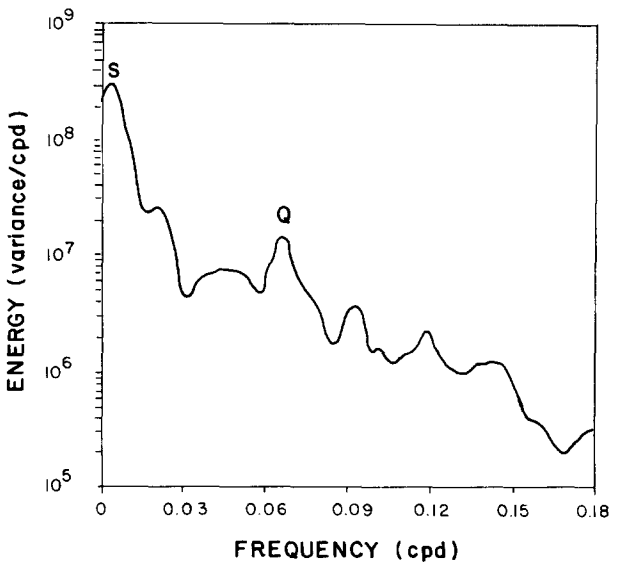

Fig. 7. Energy spectrum for the daily freshwater discharge of the Guaíba River.

level time series it was not possible to verify the response of the lagoon in the seasonal band. It is reasonable to assume that for the rainy season (winter and spring) oscillations of water level of moderate magnitude should be detected in the 8–15 days band.

5. MODEL RESULTS

The lagoon was discretized using a grid of linear triangular elements shown in Fig. 8; the bottom topography used in this model was derived from the Nautical Chart 2140 of the

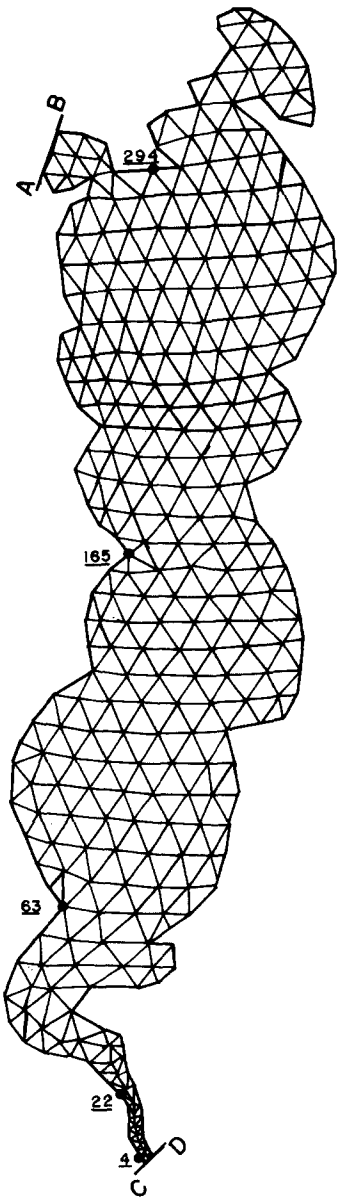

Fig. 8. Finite element grid for the Patos Lagoon. Number of nodes = 334 and number of elements = 532.

Brazilian Navy. The minimum depth used in the numerical experiments was 1.5 m. The mean latitude used in the model is 31°S. The water density and horizontal eddy viscosity coefficient were set to $\rho = 1025\ \mathrm{kg\ m^{-3}}$ and $A = 50\ \mathrm{m^{-2}\,s^{-1}}$, respectively. The integration time step is $\delta t = 60$ s and the numerical model was integrated in time for three days for all experiments. In order to reduce the effects of initialization, a time ramp of 2 h was also used to bring the wind speed from zero to its 5 m $\mathrm{s^{-1}}$ value, at the beginning of the integration.

Two types of numerical experiments were implemented for the region using the finite element barotropic model. The first set of experiments was used to investigate the lagoon's response to uniform and constant wind stress during low freshwater discharge conditions.

The river inflow discharge condition was implemented as a flow boundary condition with a magnitude of 700 $m^3 s^{-1}$ in the model nodes along the section marked A–B in Fig. 8. A second experiment was done to simulate the lagoon's response to astronomical tidal forcing implemented as a water elevation boundary condition along the section marked C–D in Fig. 8.

5.1. *Wind action*

Under normal conditions, the prevailing winds over the region are from the northeast. Immediately after the passage of a cold front, the winds blow from the southwest; 5 m s^{-1} is the typical wind speed for both conditions. Two numerical experiments were set up using these two wind field conditions. For both cases, a discharge of 700 $m^{-3} s^{-1}$ was used. This value represents the 14 year averaged summer river flow measured at Guaiba river, the main source of freshwater into the lagoon (Bordas *et al.*, 1984).

5.1.1. *Circulation in the lagoon.* Figure 9 shows the depth averaged velocity vectors for the NE wind forcing. The following features can be observed in Fig. 9(a), corresponding to 6 h of integration: the velocities are everywhere downwind; they are intensified in the central part of the lagoon where its width is reduced, showing in this area only a small lateral velocity shear. In the rest of the region, the flow is intensified near the lagoon's margins, probably due to a shallowing effect. A flow intensification towards the ocean is present in the southern extremity of the lagoon and is caused by a narrowing of the exit channel. The freshwater inflow due to the discharge of the Guaiba river is clearly seen in the northwestern portion of the lagoon.

After 72 h of NE wind forcing, the downwind flow is concentrated near the margins [Fig. 9(b)]. The model results indicate that this coastal flow is wider in the western margin. This effect seems to be associated with the more gradual bottom slope of this margin (See Fig. 1). Several vortices and upwind flows can be observed for this quasi-steady state situation. The multiple cell configuration of the lagoon seems to be the main cause of these features. The presence of such vortices has been documented by Herz (1979) through the analysis multispectral ERTS-1 images using the suspended sediments in the water as a natural tracer of the flow.

The response of the lagoon's flow, due to SW wind forcing, is displayed in Fig. 10. The main characteristics of the flow are similar to the previous case but in the opposite sense. Inflow of oceanic waters in the entrance channel and an inhibition of Guaiba river flow into the lagoon are observed. As in the previous case, the presence of vortices and wider downwind flow near the western margin can be seen in this figure. The magnitude of the surface flow is expected to be a slightly greater than the mean values shown in these figures, considering that the speed of flow decays with depth, due to the effect of bottom friction.

5.1.2. *Water level variations.* The lagoon's low frequency water level response to NE and SW winds are displayed in Fig. 11 for three sites: south (node 22; Rio Grande), mid-part (node 165; Arambaré) and north (node 294; Itapoã). As expected, the NE (SW) wind is

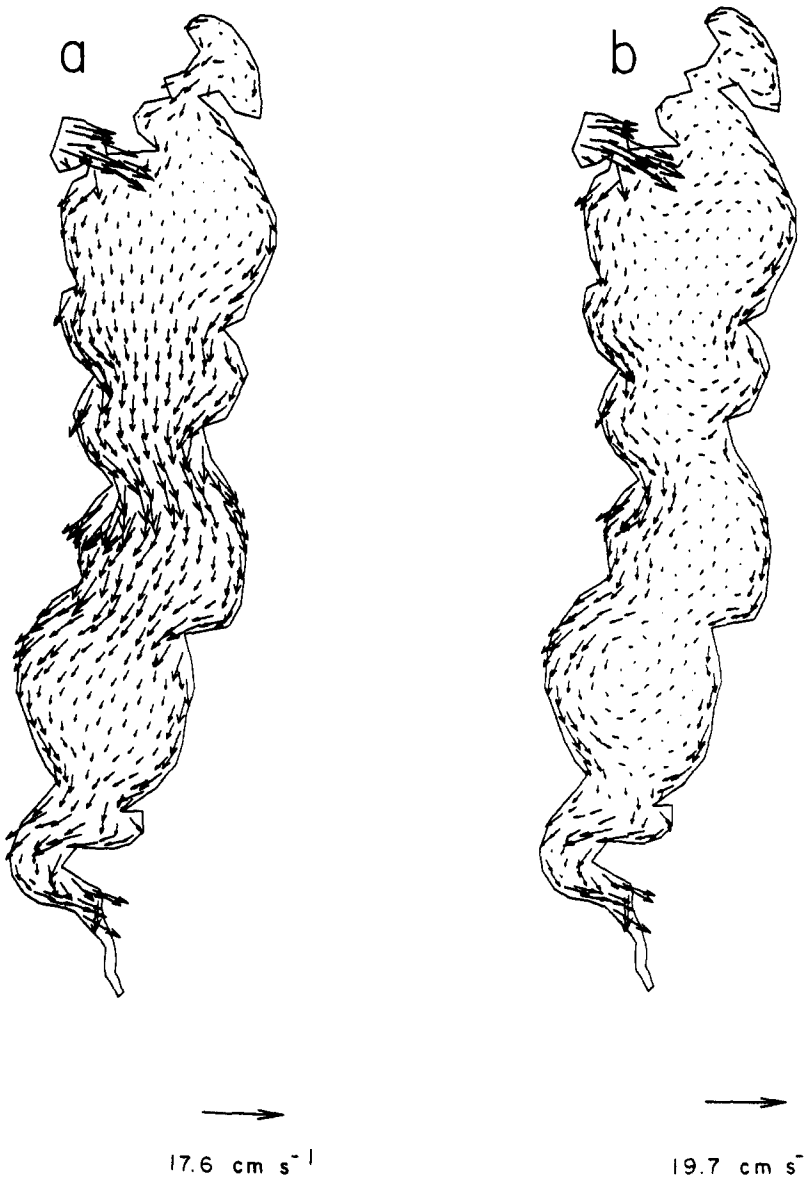

Fig. 9. Velocity vectors for the 5 m s^{-1} NE wind forcing: (a) after 6 h of integration; (b) after 72 h of integration. Due to the velocity intensification and in order to avoid confusion, near the mouth of channel the vectors were suppressed (the mean values in the channel area are about 70 cm s^{-1}).

observed to produce a water level set-up (set-down) at the southern part of the lagoon and a depression (rise) in elevation at its northern part. A 14 cm level difference between these two extremes of the lagoon is observed for steady state conditions in both cases.

The results of Fig. 11 indicate that 24 h is the time required for the steady state to be reached. At the southern and northern extremes of the lagoon, oscillations in water level with a period of 19 h are seen to be generated during the spin-up phase of the model. As

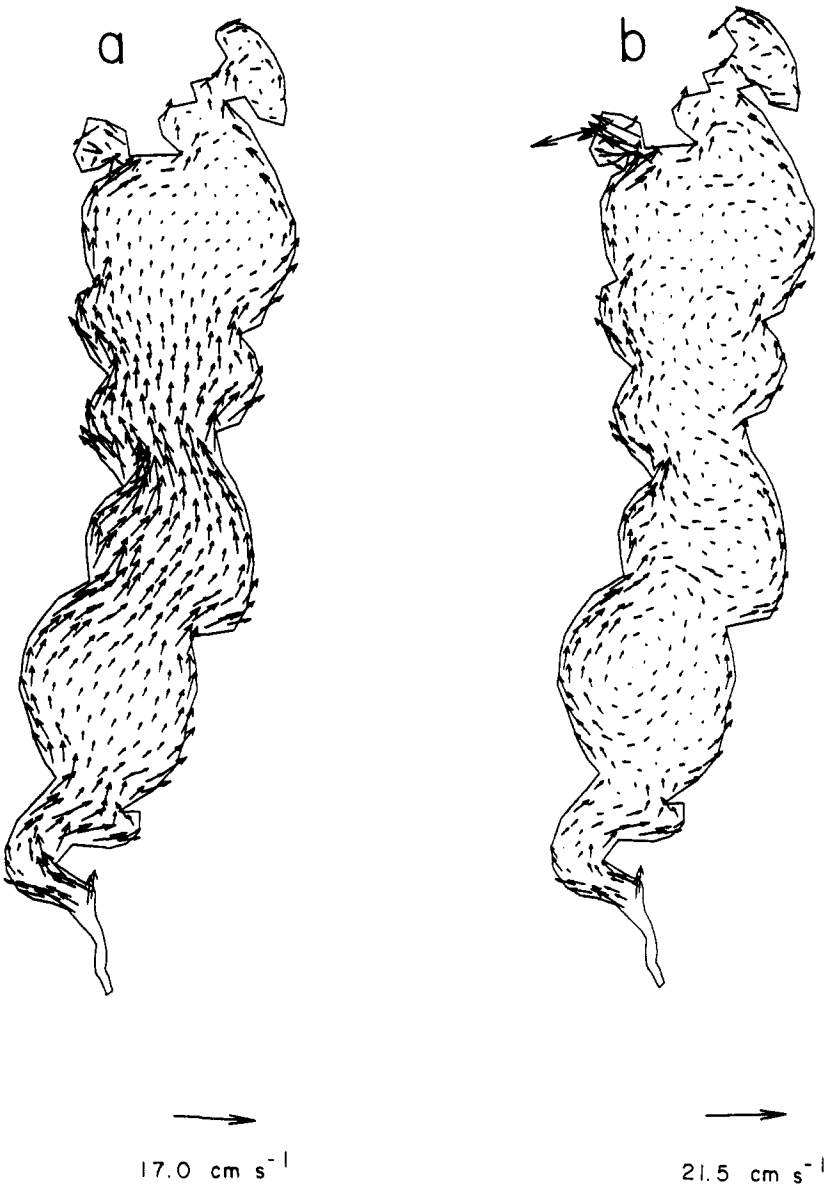

Fig. 10. Velocity vectors for the 5 m s^{-1} SW wind forcing: (a) after 6 h of integration; (b) after 72 h of integration. Due to the velocity intensification and in order to avoid confusion, near the mouth of channel the vectors were suppressed (the mean values in the channel area are about 70 cm s^{-1}).

discussed in Section 4.1, a natural period of 19.3 h is obtained through the use of Defant's method. Therefore, the oscillations present in these simulations are likely to be seiche modes of the system. In agreement with the discussion of Section 4.1, the model results also indicate that the central part of the lagoon near Arambaré behaves as a nodal zone for both seiche oscillations and set-up/set-down water level anomalies.

Although the results presented in Fig. 11(a) and (b) seem to be symmetric, a closer

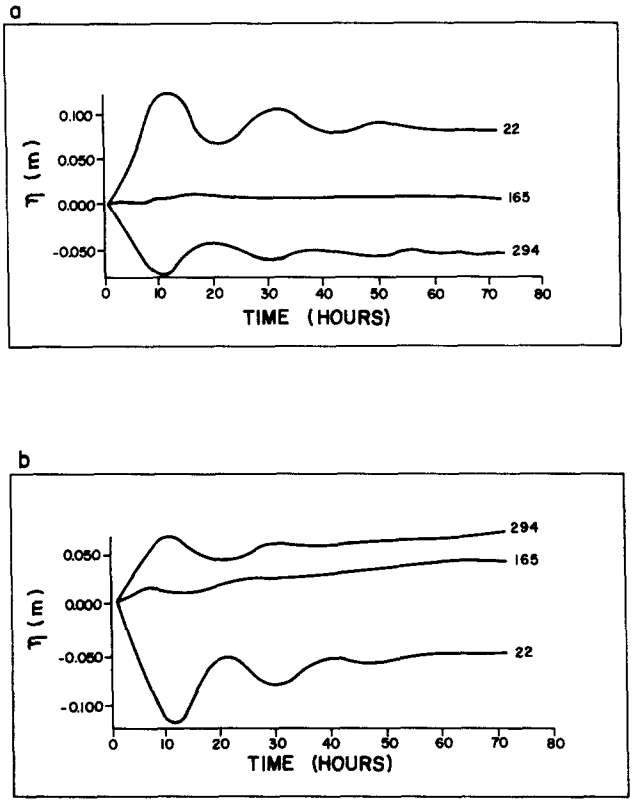

Fig. 11. Water level elevations (η) generated by the model at Rio Grande (node 22), Arambaré (node 165) and Itapoã (node 294) for the 5 m s^{-1} NE (a) and SW (b) winds.

analysis reveals that the response of the lagoon for SW wind forcing is characterized by a continuous rise of water for all nodes due to the piling up of freshwater from the Guaiba river freshwater inflow. However, this piling up of water inside of the lagoon due to southerly winds cannot last for long periods since a strong pressure gradient opposing the wind stress is eventually developed, thereby forcing a southerly upwind flow towards the ocean. This upwind flow towards the ocean has already been observed by local inhabitants.

5.2. *The astronomical tide*

In this experiment, a tidal signal and amplitude of 0.5 m was used as a boundary condition. It corresponds to the mean amplitude observed at Rio Grande. Figure 12, presenting a plot of water level for three sites along the southern portion of the lagoon, shows that the tidal amplitude is quite reduced as soon as it leaves the entrance channel. These results agree with the conclusions of Kjerfve and Magill (1989), showing that for a choked coastal lagoon, the channel acts as a low-pass filter and strongly damps out the incoming tidal signal.

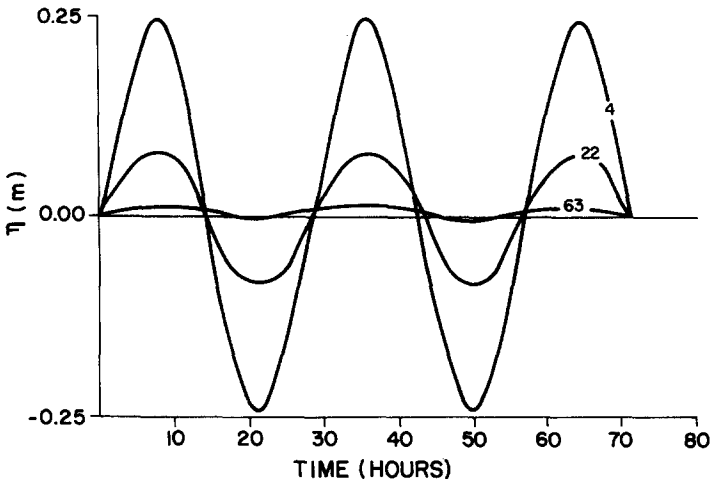

Fig. 12. Tidal elevations (η) generated by the model at three nodes located at the southern portion of the lagoon.

6. DISCUSSION AND CONCLUSIONS

The results presented in this paper indicate that the wind stress is the main factor controlling the circulation of Patos Lagoon. The longitudinal wind component acts as the main driving force, affecting not only the long period water level oscillations but also influencing the exchange of water with the adjacent continental shelf. As previously indicated, the subtidal water level oscillations were coherent with wind fluctuations in the 11 day period band associated with passage of frontal systems. Some observational studies of southern hemisphere summer mid-latitude circulation patterns, such as Randel and Stanford (1985), also have shown dominant fluctuations centered near a period of 12 days. For wintertime conditions, the analysis of Stech and Lorenzzetti (1992) shown that the dominant periodicity of the frontal passages over the southern Brazil coast is shifted towards the six day period, indicating the possibility that the subtidal oscillations would be altered accordingly.

The model results presented indicate that the longitudinal wind component blowing over the lagoon generates a typical behavior of a closed system having a nodal line at Arambaré, with the set-up/set-down at the extremities. However, the cross-spectrum analysis of the observed water level anomalies at the two extremes of the Patos Lagoon, Itapoã and Rio Grande, has not provided a phase difference of about 180° at the dominant subtidal band, as should be expected from such a mechanism. It is here conjectured that this is caused by the proximity of Rio Grande to the ocean's entrance and the consequent influence of the exchange of water with the adjacent inner shelf.

When the wind blows from the northeast (southwest), the water level set-up (set-down) should occur at the southern (northern) end of the lagoon if it was a completely closed system. However, a northeast (southwest) wind results in a coastal depression (rise) of sea-level at the adjacent continental shelf due to the Ekman transport. Therefore, near the lagoon's exit to the ocean, the coupling of the external shelf dynamics with the lagoon's interior dynamics results in opposite effects, as far as sea level anomalies are concerned, masking the set-up/set-down signal at that location. For São Lourenço, a place located at

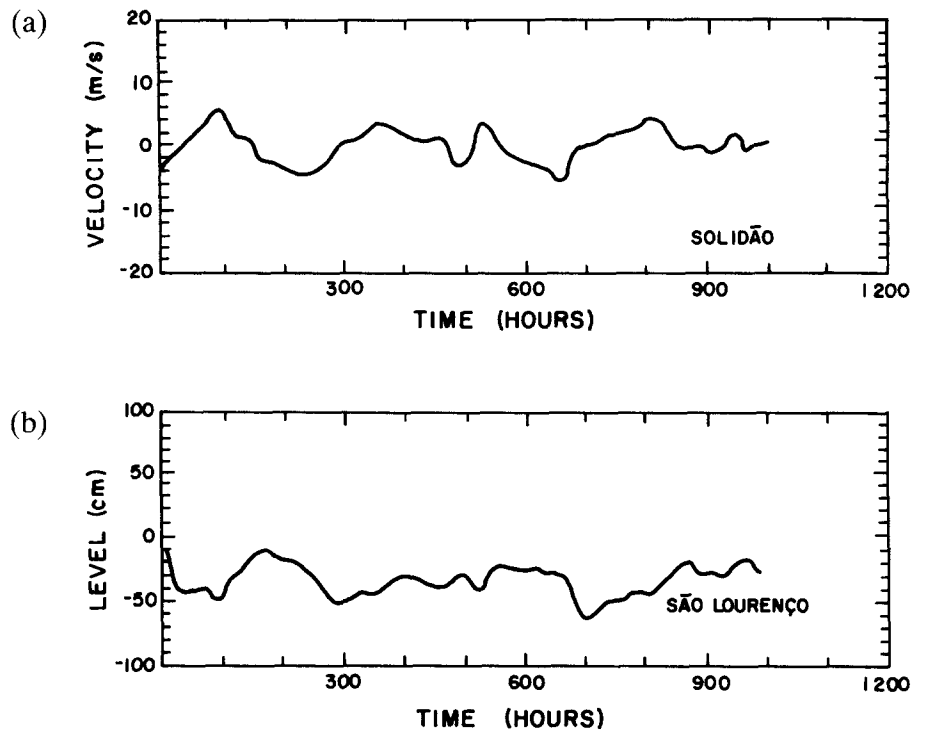

Fig. 13. Low-pass filtered time series of: (a) Solidão y-wind component; (b) São Lourenço water level.

the southern part of the lagoon but less affected by outer shelf influences, a visual inspection of Fig. 13 shows the expected 180° phase lag between longitudinal wind and São Lourenço water level.

The secondary way by which the wind influences the circulation of the Patos Lagoon is through the cross-shore sea breeze wind component. The response of the lagoon to the sea breeze forcing is easily observed in its northern region due to the absence of diurnal tidal signal which can mask this effect in the southern portions. In spite of its weaker importance with respect to the longitudinal wind effect, in the northern areas of the lagoon, and specially during summer conditions, this kind of forcing should not be disregarded. For instance, Guaiba River flow reversals have been observed during strong sea breeze events.

Freshwater discharge is another important factor in the circulation. This discharge can generate a water level head with respect to the ocean in the low frequency band of the spectrum (8–15 day period), influencing the inflow/outflow processes at the sea entrance. A model run, not presented in this paper, that used the relatively high freshwater inflow of 3000 $m^3 s^{-1}$, at the Guaiba River and a constant SW 5 ms^{-1} wind, showed an overall flow reversal and a seaward flow against the wind after the sixth day of integration, illustrating the effect of freshwater discharge.

The data analysis and model results clearly show that the tidal wave in the lagoon has its importance restricted to the region near the ocean. In spite of that, the tidal signal seems to make a strong contribution to flushing rates of properties between the lagoon and the ocean.

The following momentum balance is verified using the characteristic values obtained from model results.

(a) near-shore: $H = 1.5$ m; $v = 10$ cm s^{-1}; $(\partial\eta/\partial x) = 0.71$ cm/10,370 m; $(\partial\eta/\partial y) = 14$ cm/250,000 m

(b) mid-section: $H = 6$ m; $v = 2$ cm s^{-1}; $(\partial\eta/\partial x) = 0.22$ cm/13,689 m; $(\partial\eta/\partial y) = 14$ cm/250,000

$$-fQ_y = -gH\frac{\partial\eta}{\partial x}$$

1.13×10^{-5}	1.01×10^{-5}	near-shore,
0.91×10^{-5}	0.95×10^{-5}	mid-section,

$$0 = -gH\frac{\partial\eta}{\partial y} + \frac{1}{\rho}\tau_{wy} - \frac{1}{\rho}\tau_{by}$$

0.82×10^{-5}	-0.33×10^{-4}	0.23×10^{-4}	near-shore
0.33×10^{-4}	-0.33×10^{-4}	0.09×10^{-4}	mid-section.

Therefore, in the lateral direction, a geostrophic balance is observed both at shallow and deeper parts of the lagoon. For the deeper parts, a wind set-up/set-down equilibrium in the longitudinal direction is observed with the pressure gradient balancing the wind stress. For nodes located near the shores the momentum balance is predominantly frictional, with the wind stress being opposed mainly by the bottom friction and with a secondary contribution of the pressure gradient. All the remaining terms, not shown, are negligible compared with the ones presented.

Although the results presented in this paper are more representative of quasi-steady state conditions, they still should represent quite well the overall aspects of the dynamics of this water body. Considering that only one day is necessary for the steady state to be reached and that the average period between fronts is about 11 days, it can be concluded that most of the time the lagoon system should not be too far from a quasi-steady state configuration. It should be noted, also, that the transient states associated with passage of cold fronts generally last only about 12 h since the mean frontal propagation speed is of the order of 500 km day^{-1} (Stech and Lorenzzetti, 1992).

Finally, it must be emphasized that this study should be considered as a first order approximation of the general aspects of the Patos Lagoon circulation. The southern area of this water body shows a typical behavior of an estuarine environment, with three-dimensional circulation patterns. Therefore, to better describe the dynamics of this part of the lagoon, a three-dimensional and thermodynamically active model needs to be implemented.

Acknowledgements—The authors wish to thank the Interministerial Commission for Marine Resources (CIRM) and the Rio Grande do Sul Research Supporting Foundation (FAPERGS) for their support of the PLP (CIRM) and PLATES (FAPERGS—90.1220.0) projects; Walter H. Pinaya, Celso B. Miranda and André L. Belém for helping in the model implementation; Rogério Dewes of DNAEE for providing the river water levels; and last, but not least, Dr Merritt R. Stevenson of INPE, for his suggestions.

REFERENCES

Bordas M. P., A. Borche Casalas, A. L. de Silveira and M. R. R. Gonçalves (1984) *Circulação e dispersão em sistemas costeiros e oceânicos, caso da Lagoa dos Patos*. Technical Report, Instituto de Pesquisas Hidráulicas, UFRGS, Brazil.

Calliari L. J. (1980) Aspectos sedimentológicos e ambientais na Região Estuarial da Lagoa dos Patos. M.Sc. Thesis, CECO/UFRGS, Brazil, 189 pp.

Cameron W. M. and D. W. Pritchard (1963) Estuaries. In: *The sea*, M. N. Hill, editor, Wiley, New York, pp. 305–324.

Closs D. (1962) Foraminíferos e tecamebas na Lagoa dos Patos. *Boletim da Escola de Geologia*, Universidade Federale Rio Grande do Sul, Brazil, **11**, 1–30.

Defant F. (1961) *Physical Oceanography*, Pergamon Press, London, 729 pp.

Herz R. (1977) Circulação das águas de superfície da Lagoa dos Patos. D.Sc. Thesis, Universidade de São Paulo, Brazil, 312 pp.

Herz R. (1979) Spatial and temporal variations in lagoon and coastal processes of the southern Brazilian coast. *Proceedings of the XIII International Symposium on Remote Sensing of Environment*, **43**, 1643–1656.

Hickey B. M. and P. Hamilton (1980) A spin-up model as a diagnostic tool for interpretation of current and density measurements on the continental shelf of Pacific Northwest. *Journal of Physical Oceanography*, **10**, 12–24.

Jacob G. and J. K. Kazimier (1989) Curva-chave: análise e traçado. Technical Report DNAEE, Brazil, 273 pp.

Kjerfve B. (1986) Comparative oceanography of coastal lagoons. In: *Estuarine Variability*, D. A. Wolfe, editor, Academic Press, New York, pp. 63–81.

Kjerfve B. and K. E. Magill (1989) Geographical and hydrodynamic characteristics of shallow coastal lagoons. *Marine Geology*, **88**, 187–199.

Lorenzzetti J. A. (1976) Aplicação da técnica de análise espectral cruzada ao estudo da correlação entre as oscilações do nível do mar observadas em Cananéia e Bom Abrigo. M.Sc. Thesis. IOUSP/USP, Brazil, 118 pp.

Malaval M. B. (1922) *Travaux du port et des la barre de Rio Grande, Bresil.* Paris, Eirolles Editeurs.

Moller O. O. Jr., P. S. G. Paim and I. D. Soares (1991) Facteurs et mecanismes de la circulation des eaux dans l'estuarie de la Lagune dos Patos (RS, Bresil), *Bulletin de Institut de Geologie Bassin d'Aquitaine*, Bordeaux, **449**, 15–21.

Motta V. F. (1969) Relatório–diagnóstico sobre a melhoria e o aprofundamento do acesso pela barra do Rio Grande. *Inst. Pesq. Hidráulicas*, Universidade Federal do Rio Grande do Sul, Brazil, 114 pp.

Orlanski I. (1976) A simple boundary condition for unbounded hyperbolic flows. *Journal of Computational Physics*, **21**, 251–269.

Randel W. J. and J. L. Stanford (1985) An observational study of medium-scale wave dynamics in the southern hemisphere summer. Part I: Wave structure and energetics. *Journal of Atmospheric Sciences*, **442 (11)**, 1172–1188.

Stech J. L. and J. A. Lorenzzetti (1992) The response of the South Brazil Bight to the passage of wintertime cold fronts. *Journal of Geophysical Research*, **497(C6)**, 9507–9520.

Wang J. D. and J. J. Connor (1975) Mathematical modeling of near coastal circulation. Technical Report 200, R. M. Parsons Laboratory, Massachussetts Institute of Technology, Cambridge, MA, U.S.A.

Ulrich T. J. and T. N. Bishop (1975) Maximum entropy spectral analysis and autoregressive decomposition. *Review of Geophysics and Space Physics*, **413, 1**, 183–200.